FRET Probes in Micellar Systems: Micelle Formation Indicator and the Enzymes Catalytic Activity Signal Enhancer

Igor Dmitrievich Zlotnikov , Ivan V. Savchenko , Elena Vadimovna Kudryashova *

Posted Date: 6 December 2023

doi: 10.20944/preprints202312.0409.v1

Keywords: FRET probes; rhodamine 6G; reversed micelle; surfactants; enzyme activity

Article

FRET Probes in Micellar Systems: Micelle Formation Indicator and the Enzymes Catalytic Activity Signal Enhancer

Igor D. Zlotnikov, Ivan V. Savchenko and Elena V. Kudryashova *

Faculty of Chemistry, Lomonosov Moscow State University, Leninskie Gory, 1/3, 119991 Moscow, Russia; zlotnikovid@my.msu.ru (I.D.Z.); ivan.savchenko@chemistry.msu.ru (I.V.S.)

* Correspondence: helenakoudriachova@yandex.ru

Abstract: Fluorescent labels, especially FRET probes, are promising tools for studying a number of biochemical processes. In this paper, we promoted 2 important applications of FRET probes (MUTMAC-R6G and FITC-R6G): i) the formation of micelles from surfactants of various natures and polymers (chitosan – fatty acid), as well as ii) monitoring of enzymatic activity with improved parameters (increased analytical signal and improved selectivity due to shift to the long-wavelength region). The formation of micelles is accompanied by the convergence of fluorophores in the hydrophobic micelle core by a distance closer than in the buffer solution, thus r/R_0 (where R_0 – Foerster radius) is chosen as an analytical signal of micelle formation, including critical micelle concentration (CMC) and critical pre-micelle concentration (CPMC). The CMC values calculated using FRET probes are in a good agreement with literature data. At the same time, the r/R_0 function provides valuable information about the nature and mechanism of micelle formation. With the second analytical application of FRET probes, we considered the optimization of techniques for studying enzymatic activity. The enzyme catalyzes the reaction with the release of a fluorescent product, the signal from which may not be enough for detection, or it may be quenched, for example, in the reverse micelles (AOT-octane). Here we have proposed a solution – a FRET probe containing a rhodamine 6G (R6G) acceptor, which allows us to monitor the enzymatic reaction selectively (in the red region, 550-600 nm), and obtain a significantly higher fluorescence yield (potentially from 10 to 250 times). Thus, we have demonstrated a high potential for the FRET probes application as indicators of micelle formation as well as for the study of the enzyme catalytic activity. In the future, the method developed has prospects for application in the visualization of the enzyme functioning in cells due to the shift of the fluorescence signal to the long-wavelength region with an increase in the signal selectivity to suppress autofluorescence.

Keywords: FRET probes; rhodamine 6G; reversed micelle; surfactants; enzyme activity

1. Introduction

Last decade Förster resonance energy transfer (FRET) between fluorophore molecules, have been actively developing as quantitative approach to determine a number of biochemical parameters in real time [1]. This approach turned out to be advantageous, providing high sensitivity and selectivity, since the FRET effect reflect the specific molecular organization in the system. In addition, changes in the FRET signal can be monitored online upon supramolecular assembles self-organization process, which is an undoubted advantage over other methods such as electron microscopy, radioactive tagging and dynamic light scattering. It is worth noting that the FRET signal can be used to create powerful sensors in the biological research and medical applications.

FRET can be observed when the emission spectrum of the donor overlaps with the excitation spectrum of the acceptor, and the distance of energy transfer can occur is limited to ~10 nm. The quantum yield of this energy-transfer transition, FRET efficiency (E) is determined by the donor-to-acceptor distance r [1–6]:

 doi:10.20944/preprints202312.0409.v1

$$E = 1 / (1 + (r/R_0)^6), \quad (1)$$

where R_0 is the Förster distance of the given pair donor-acceptor, which can range from 10 to 100 Å.

Since even small changes in the donor-acceptor distance (r/R_0) crucially affect FRET efficiency, FRET-based approach can be considered as a powerful tool for the studies involving accurate estimation of the inter- and intramolecular distances, in the molecular dynamics assays, molecular interactions and binding events. In this paper we investigated the role of the micelles formation in FRET phenomenon, where FRET- effect is expected to be increased due to concentration and convergence of the donor-acceptor agents caused by its specific hydrophobic-hydrophilic phase distribution in micelles. So, two main applications of FRET probes are considered: 1) determination of the micelles formation, 2) improved method of the enzymatic activity detection in the model biologically related systems.

In the case of classical micelles the spontaneous formation of spherical particles associates of surfactant molecules (SDS, Triton X-100, etc) leads to the loading of the aromatic fluorophore molecules into the hydrophobic micelle core, which can be used in the observation of FRET during micelle formation [2]. Recently we suggested the approach where FRET was used as an effective tool for monitoring the formation of polymeric micelles [3] or micro-/nano-gels [1]. The study of micelle formation is important from the point of view of creating smart delivery systems for antibacterial and antitumor drugs [4–17].

FRET can be useful for tracking drug release and it is potentially applicable for determining the drug localization and cells permeability, for example, in cytostatic effect studies on a tumor cells [18]. In addition, FRET is applicable for studying the formation of various types of nanoparticles based on polymers (chitosan, chitosan-PEG) and proteins (ovalbumin, casein, etc.) [19]. Nanoparticles, along with micelles, deserve special attention as promising drug carriers [20–33].

In this work, we used FRET probes to study the activity of enzymes of different class (chymotrypsin, asparaginase, phosphatase) in a system of reversed micelles in which fluorophore molecules are close to each other due to the small volume of the aqueous phase in comparison with an aqueous solution system. An interesting phenomenon based on the FRET effect is observed: the enzyme catalyzes a reaction in which a fluorophore- donor is released, providing the ignition of fluorescence of a fluorophore-acceptor (rhodamine 6G with its fluorescence at 550-600 nm), which has a 1-2 orders of magnitude higher fluorescence emission coefficient. Thus, this allowed us to observe the reaction in the red region selectively and with much higher signal value.

This approach can be used both to study the catalytic activity of enzymes in micelles, (as relevant model of biomembrane system) and further it can be applied to visualize the enzyme functioning in the living cells in the condition of their localization in specific cellular structures with for example CLSM technique, where fluorescent probes in the visible area are required with high resolution and signal selectivity (to exclude the autofluorescence).

2. Materials and Method

2.1. Reagents

Surfactants SDS (sodium dodecyl sulfate), Triton X-100 and zephirol (N-benzoyl-N,N-dimethyldodecan-1-ammonium chloride) were purchased from Reachim (Moscow, Russia). The fluorophores rhodamine 6G (R6G), fluorescein isothiocyanate (FITC), 4-methylumbelliferyl p-trimethylammoniocinnamate chloride (MUTMAC), 4-methylumbelliferyl phosphate (MUmb-phosphate), 4-methylumbelliferone (MUmb), L-aspartic acid β-(7-amido-4-methylcoumarin), chitosan oligosaccharide lactate 5 kDa (Chit5), lipoic acid (LA), 1-ethyl-3-(3-dimethylaminopropyl) carbodiimide (EDC), N-hydroxysuccinimide (NHS) were purchased from Sigma-Aldrich (St Louis, USA).

Enzymes: α-chymotripsin from bovine pancreas (EC 3.4.21.1, ≥40 units/mg protein), acid phosphatase (EC 3.1.3.2), alkaline phosphatase (EC 3.1.3.1) – were purchased from Sigma-Aldrich (St.

 doi:10.20944/preprints202312.0409.v1

Louis, MI, USA). The enzyme *Erwinia carotovora* asparaginase (EwA) was isolated and purified as described by us earlier [34,35]. The activity of asparaginase was checked using the method of circular dichroism spectroscopy on device J-815 CD spectrometer (Jasco, Tokyo, Japan).

2.2. Synthesis of chitosan grafted with lipoic acid (Chit5-LA)

The synthesis of modified chitosan was carried out as described by us earlier with some modifications [36–38]. Chitosan was dissolved in 1 mM HCl solution (10 mg/mL) and then the pH was adjusted to 7.4 using 0.1 M phosphate buffer. Lipoic acid was dissolved in PBS/EtOH (50/50 v/v) to a concentration of 20 mg/mL. NHS and EDC were dissolved in EtOH (50 mg/mL). The crosslinking reaction was carried out using a carbodiimide approach, for which the solutions described above were mixed so as to obtain the Chit5 / LA / EDC / NHS mass ratios = 1 / 0.33 / 3 / 1. The mixture was incubated for 6 hours at a temperature of 50 °C. The product was then purified by three-stage dialysis against water (12h×3, cut-off 3.5 kDa). The polymer was freeze-dried at –70 °C.

2.3. Characterization of chitosan grafted with lipoic acid (Chit5-LA)

The characterization of chitosan grafted with lipoic acid (Chit5-LA) was carried out by the methods of FTIR, ^{1}H NMR spectroscopy, atomic force microscopy and circular dichroism spectroscopy.

FTIR spectra of Chit5, LA, Chit5-LA were recorded using a FTIR microscope MICRAN-3 and Bruker Tensor27 spectrometer equipped with a liquid-nitrogen-cooled MCT (mercury cadmium telluride) detector, as described earlier [36,39]. The Chit5 and LA chemical conjugation was confirmed by shifts of the absorption band of carboxylic acid group (1730–1770 cm^{-1}) of lipoic acid to the low-frequency region due to the formation of amide bonds between chitosan NH_2 group and COOH group of LA: 1500–1600 cm^{-1} (amide –NH–) and 1640–1720 cm^{-1} (–C(=O)–).

^{1}H NMR spectroscopy was confirmed chemical structure of Chit5-LA conjugate. Chemical shifts (δ, ppm) for Chit5 were observed: 4.22 (H1), 3.23 (H2), 3.79, 3.96 (H3, H4, H5, H6, H6′), 2.11 (NH–C(=O)–CH_3). Chit5-LA-20 ^{1}H NMR spectra contain signals of chitosan indicated above, increased signals at 2.0–2.3 ppm, 1.25 ppm that were assigned to N-alkyl groups of LA, and signals of 3.64 ppm (C–H near the dithiolane fragment) and 2.3 ppm (β–H with relation to the carboxyl group) assigned to LA in polymer [36].

Circular dichroism spectroscopy was used to calculate the degree of deacetylation in Chit5, which amounted to 92%.

Atomic force microscopy (AFM microscope NTEGRA II) was used to visualize polymeric micelles based on grafted chitosan and compare it in terms of shape and size with non-modified chitosan.

2.4. FRET probes for determination of CMC for micelles formed from surfactants and Chit5-LA

FRET probes are two pairs of fluorophores FITC-R6G and MUTMAC-R6G, where both R6G is acceptor. We chose surfactants zephirol, Triton X-100, SDS and chitosan grafted with lipoic acid (Chit5-LA) as amphiphilic compounds for studying micelles formation.

The excitation and emission spectra of fluorescence were recorded on the device Varian Cary Eclipse fluorescence spectrometer (Agilent Technologies, Santa Clara, CA, USA). For FRET probe 1 (MUTMAC+R6G) λ_{exci} = 360 nm, λ_{emi} = 450 nm (donor) and 550 nm (acceptor) were used. For FRET probe 2 (FITC+R6G) λ_{exci} = 460 nm, λ_{emi} = 520 nm (donor) and 550 nm (acceptor) were used.

The final concentration of fluorophores was 1 μg/mL. Fluorophore emission and excitation spectra were recorded for each separately and for a donor+acceptor mixture in a buffer solution (PBS 0.01M, pH 7.4) in the absence of surfactants and in its presence of various amounts.

FRET efficiency E was calculated as $E = 1 - F_{DA}/F_D$ **(2)** for MUTMAC+R6G pair and as $E = F_{AD}/F_A - 1$ **(3)** for FITC+R6G pair. Where F_{DA} and F_D – the intensities of donor fluorescence in the presence

 doi:10.20944/preprints202312.0409.v1

and absence of the acceptor, respectively; F_{AD} and F_A – the intensities of acceptor fluorescence in the presence and absence of the donor, respectively.

The ratio r/R_0 was calculated as an analytical signal of micelle formation; $r/R_0 = (1/E - 1)^{(1/6)}$ **(4)**, where r is the distance between donor and acceptor and R_0 is Förster radius. Critical micelle concentration (CMC) was estimated using x-coordinate of a point on the right branch of the graph (r/R_0 versus surfactant concentration) with the value r/R_0 equal to the initial one (for a pair of fluorophores in a buffer solution without surfactants).

The formation of S-S bonds between Chit5-LA polymeric chains was studied using FRET probes, registering their fluorescence as described above. First, dithiothreitol was added to the self-assembled Chit5-LA samples (0.05 mg/mL) to the final concentration of 0.2 mg/mL, incubated for 30 minutes at 37 °C, followed by oxidized glutathione GSSG addition to the final concentration of 2-5 mg/mL. The fluorescence values were recorded before and after the addition of each component.

2.5. Enzyme studies

To make a solution of reversed micelles with a given hydration degree (W_0), a certain amount of PBS buffer solution (Vaq) was added to 1 mL of micellar solution (Vmic) based on the formula $Vaq = 18 * C_{AOT} * W_0$ (μL), where C_{AOT} is the concentration of AOT equal to 0.1 M. The resulting mixture was vigorously shaken until a homogeneous optically transparent solution was formed.

The catalytic activity of enzymes was determined fluorometrically on the device Varian Cary Eclipse fluorescence spectrometer (Agilent Technologies, Santa Clara, CA, USA). The reaction rate was measured by the accumulation of the fluorescent reaction product and R6G FRET agent: specific parameters are indicated in the captions to the tables and figures.

3. Results and Discussion

3.1. Article design

The present work is aimed at studying the applications of the FRET effect as a selective indicator of a number of bio-chemical events. We consider the formation of micelles from surfactants of different structure (cationic, anionic and neutral) and modified polymers (chitosan grafted with fatty acid), where FRET occurs between two fluorophores pairs (R6G with MUTMAC or FITC) due to their convergence in the core of the micelle. Second aspect under consideration is that micellar enzymology is interesting areas in which the FRET could help to modify existing techniques or to monitor the certain reaction mechanisms in a new way. So, we propose to determine the enzymatic activity using FRET technique: the enzyme catalyzes a reaction where a fluorophore donor is released (MUmb). Due to the FRET this provides the ignition of fluorescence of a fluorophore – acceptor (R6G), which has a 1-2 orders of magnitude higher fluorescence emission coefficient, which allowed us to observe the reaction in the red region selectively and with high the value of the signal. Thus, it could provide more selective visualizing the enzyme functioning in cells compartments and cellular structures visualization for example with confocal laser scanning microscope technic.

Objects of research (Figure 1): i) two pairs of fluorophores FITC-R6G and MUTMAC-R6G; ii) surfactants zephirol, Triton X-100, SDS; iii) Chitosan grafted with lipoic acid, iv) enzymes: chymotrypsin, acid and alkaline phosphatase, L-asparaginase catalyzing the hydrolysis reaction of the MUmb- or coumarin- derivatives with the formation of fluorophores - donor, which could increase the fluorescence of the R6G (acceptor) due to FRET.

Preprints (www.preprints.org) | NOT PEER-REVIEWED | Posted: 6 December 2023 doi:10.20944/preprints202312.0409.v1

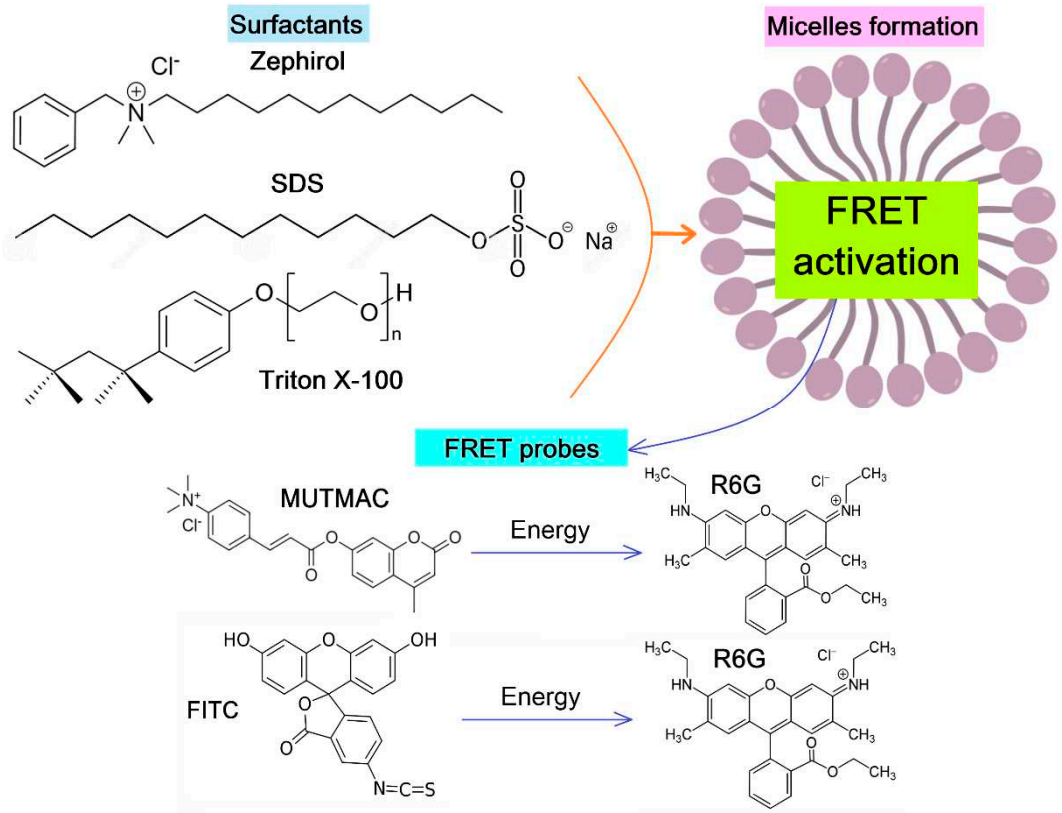

(a)

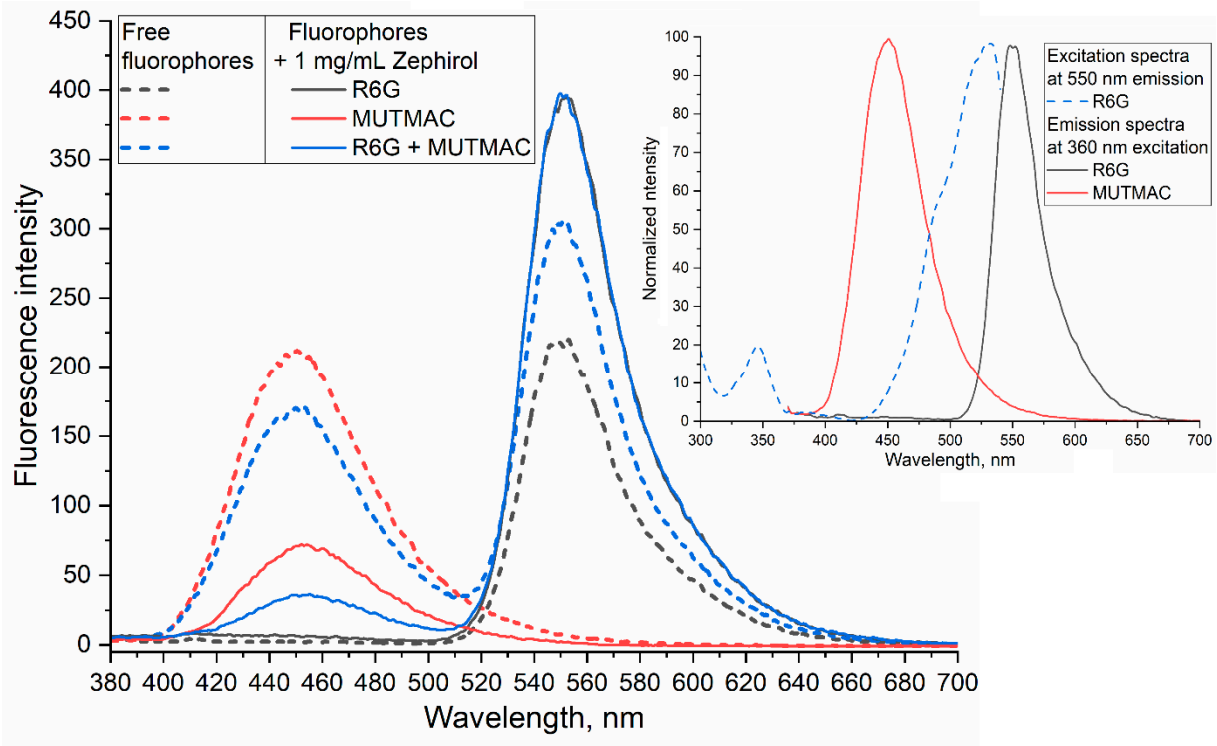

(b)

Preprints (www.preprints.org) | NOT PEER-REVIEWED | Posted: 6 December 2023 doi:10.20944/preprints202312.0409.v1

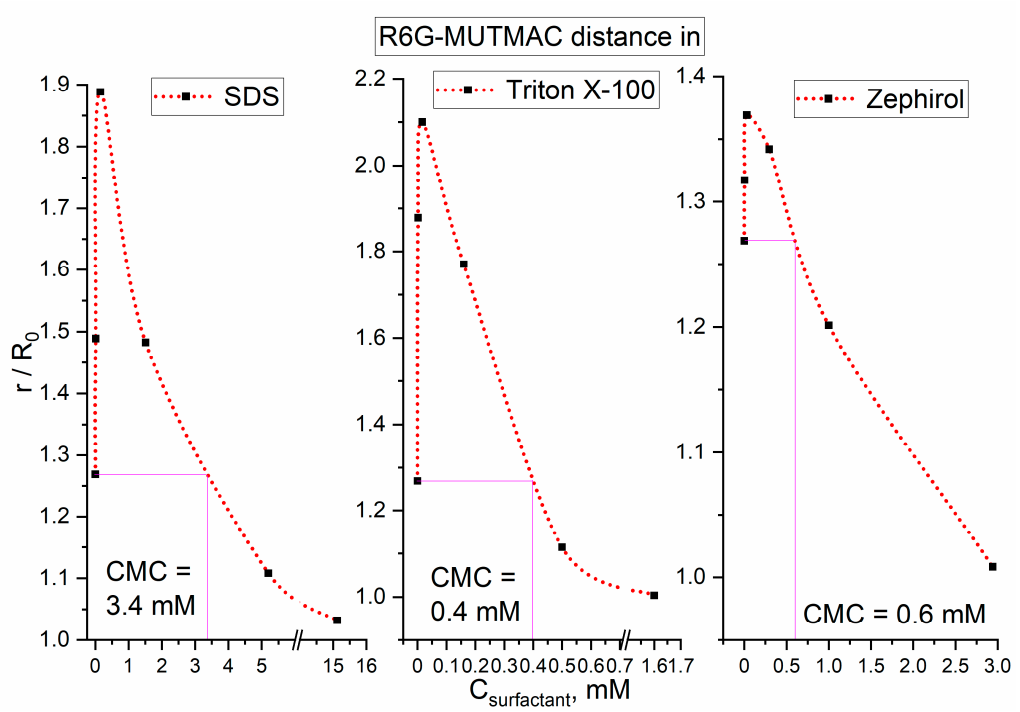

(c)

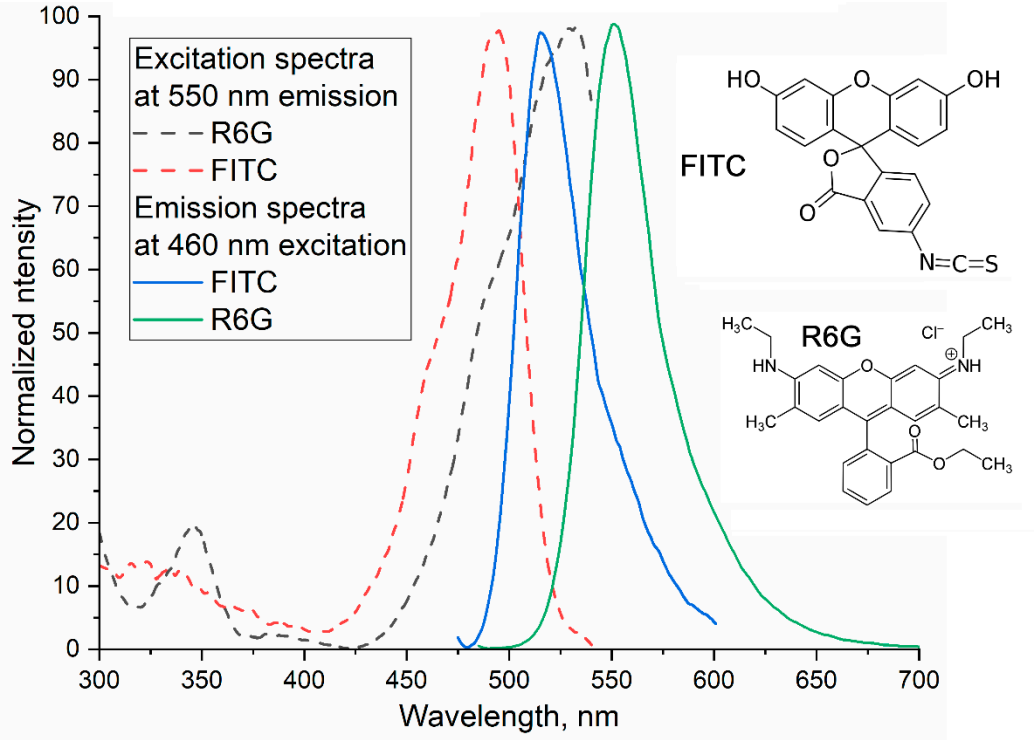

(d)

Preprints (www.preprints.org) | NOT PEER-REVIEWED | Posted: 6 December 2023 doi:10.20944/preprints202312.0409.v1

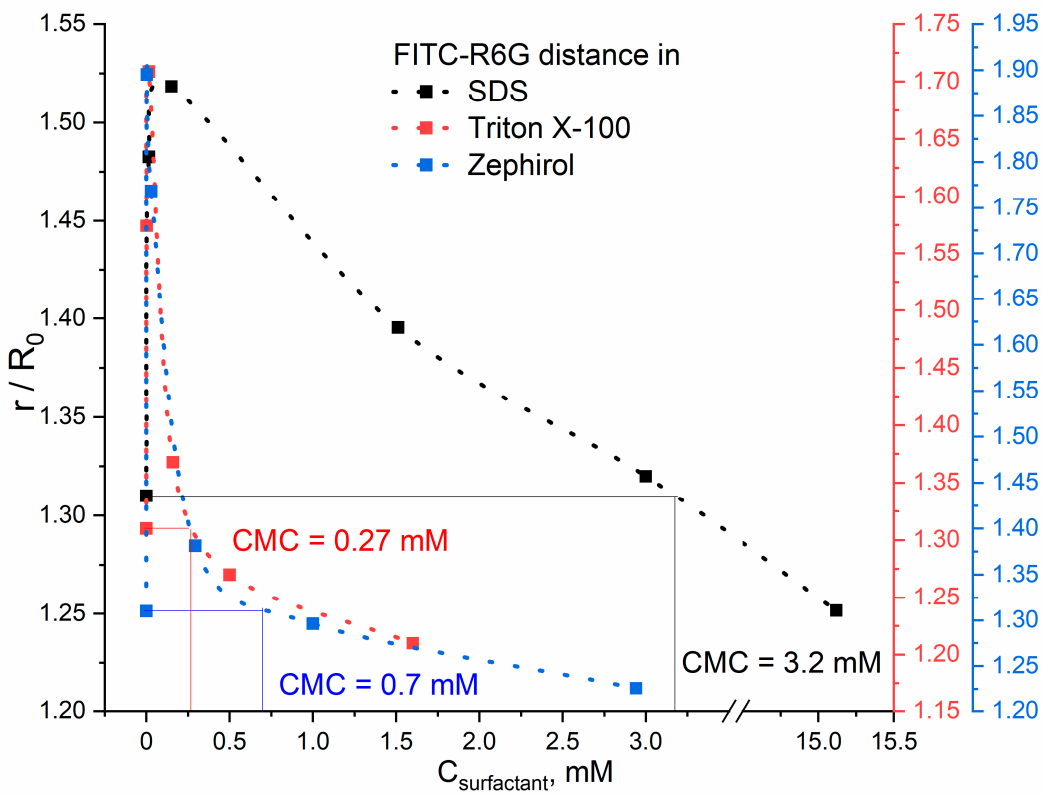

(e)

Figure 1. (a) Experiment design: FRET as an indicator of micelle formation from surfactants. **(b)** Emission fluorescence spectra of MUTMAC, R6G alone and its mixtures 1 to 1 (mol/mol) in PBS buffer solution (0.01M, pH 7.4) and in the presence of 1 mg/mL of the surfactant zephirol. The excitation wavelength is 360 nm. The insert shows the excitation and emission spectra of these fluorophores in PBS. **(c)** The dependences of r/R₀ (MUTMAC-R6G) on the surfactants' concentration. r is the distance between donor and acceptor and R₀ is Förster radius. **(d)** The excitation and emission spectra of FITC and R6G fluorophores in PBS at excitation wavelength 460 nm. **(e)** The dependence of r/R₀ (MUTMAC-R6G) on the surfactants' concentration. r is the distance between donor and acceptor and R₀ is Förster radius. T = 22 °C.

3.2. FRET as an indicator of micelle formation in surfactants solution

As pairs of fluorophores with the FRET function, we chose MUTMAC-R6G and FITC-R6G (Figure 1a). The first pair is appropriate in terms of the ratio of the fluorescence intensities of the donor and acceptor (approximately 1 to 1), as well as the visual separation of emission peaks. The second pair: visually the fluorescence peaks are not well resolved into components due to the close location of the bands of donor emission and acceptor absorption, however, this determines the high efficiency of FRET (E value (eq. 1)). Such variability (spatial resolution) / (FRET efficiency) was studied here to select the optimal pair of fluorophores with the FRET function.

3.2.1. MUTMAC – R6G pair

Figure 1b shows the excitation and emission fluorescence spectra of MUTMAC (donor) and R6G (acceptor). The main components are the fluorescence peak of the donor at 450 nm and the acceptor - at 550 nm. The excitation wavelength was 360 nm, so that, both MUTMAC and partially R6G will be excited, which makes it possible to monitor the fluorescence of both fluorophores. To quantify the formation of micelles from surfactants, it is necessary to select the target signal: the most pronounced is FRET efficiency (E value – equations 1-3) and the ratio r/R₀ (eq. 4), characterizing the distance

Preprints (www.preprints.org) | NOT PEER-REVIEWED | Posted: 6 December 2023 doi:10.20944/preprints202312.0409.v1

between two molecules of the fluorophore-donor and acceptor. r/R_0 is directly related to the formation/disaggregation of micelles: 1) the addition of small amounts of surfactant to the system leads to the increasing the donor-acceptor molecules distance (Figure 1c); 2) the formation of micellar structures is reflected in the convergence of fluorophores due to its incorporation into the hydrophobic core of micelles, enhancing with the increase in surfactants concentrations. So, the dependences of r/R_0 on surfactants' concentrations has a maximum, which means initial process of the surfactant molecule aggregation (pre-micelles). The critical pre-micelle concentration (CPMC) can be determined from the position of the maximum curve. However, another analytically significant parameter is the critical micelle concentration (CMC). In this case, the CMC corresponds to a point on the right branch of the graph with the value r/R_0 equal to the initial one (for a pair of fluorophores in a buffer solution without surfactants) – Figure 1c.

3.2.2. FITC – R6G pair

Figure 1d shows the excitation and emission fluorescence spectra of FITC (donor) and R6G (acceptor) separately from each other in a buffer solution. The main components are the fluorescence maximum for the donor is observed at 520 nm and at 550 nm for the acceptor. The excitation wavelength was 460 nm – for the selective observation of the FITC emission peak. In this system, it is most informative to determine the r/R_0 ratio by the igniting of the acceptor (R6G) fluorescence intensity. Similarly to MUTMAC – R6G pair considered above, the dependences of r/R_0 on $C_{surfactant}$ with a maximum are obtained for FITC – R6G pair. Graphically the points corresponding to CMC are marked on the Figure 1e.

3.2.3. Comparison of CMC obtained using two FRET probes and literature data

Based on the plots given in Figure 1b,d (distances between the fluorophore-donor and acceptor plotted on the concentration of surfactants'), the CMC values were graphically determine (the results are presented in Table 1). The data obtained using two FRET probes coincide within the margin of error and satisfy the literature data. This means that the technique of FRET probes allows us to study the mechanisms of micelle formation and determine not only CMC, but also CPMC, which was previously available only by NMR spectroscopy.

Table 1 shows the CMC values determined using the FRET probe technique. The highest CMC value is typical for surfactants with a low molecular weight – SDS, an order of magnitude lower CMC values are typical for surfactants with a high molecular weight: Triton X-100 and Zephirol – due to multipoint interactions. The effect of the surfactants charge on the CMC is rather pronounced: the smallest CMC values are characteristic for uncharged surfactants. At the same time, the Triton X-100 is characterized by a higher aggregation degree of 143 versus 50 for SDS [40,41]. This is reflected in increase in the sharpness of the peak r/R_0 vs $C_{surfactant}$, which indicates the sensitivity of the presented FRET probes.

However, the question of the quantitative distribution of fluorophores inside and outside the micelles remains open: the answer will be given when using enzymatic techniques in section 3.3.

Table 1. Critical micelle concentrations (CMCs), critical pre-micelle concentrations (CPMCs) for surfactants determined using FRET probes in comparison with the literature data. PBS (0.01M, pH 7.4). T = 22 °C.

Surfactant	**CPMC, μM**	**CMC, mM**		
		FRET probe 1: MUTMAC +R6G	FRET probe 2:	Literature data

Preprints (www.preprints.org) | NOT PEER-REVIEWED | Posted: 6 December 2023 doi:10.20944/preprints202312.0409.v1

			FITC+ R6G	
SDS (sodium dodecyl sulfate)	15± 4	3.4±0.2	3.2±0.2	3.32±0 .01 [42]
Triton X-100	16± 3	0.39±0.06	0.27±0. 04	0.3±0. 01 [42]
Zephirol (benzalko nium chloride)	4±1	0.6±0.1	0.7±0.1	0.02% (0.6 mM) [43]

3.2. Formation of polymeric micelles with indicated by FRET probes

To show the versatility of FRET approach to determine CMC, in addition to surfactants micelles we studied polymeric micelles based on the chitosan (5 kDa) grafted with lipoic acid (Chit5-LA, Figures S1 and S2). Figure 2a shows the distance between the fluorophores pair (donor-acceptor) plotted as a function of the grafted chitosan molecules concentration. The CMC calculated for Chit5-LA is 16 nM, which is in a good agreement with the data described earlier for similar systems [36].

The developed FRET-based approach is further applied to study of the mechanism and the kinetics of polymer micelles formation. Of particular interest is the aspect of the formation of the polymeric micelles (as a smart drug delivery system), where the kinetics data of formation/destruction of S-S bonds are of great importance. This can be considered as the basis for creating stimulus-sensitive drug delivery systems to tumor cells, where drug molecules will be selectively released due to the higher glutathione level in cancer cells [36,38].

So, based on chitosan-lipoic acid conjugates (Figure 2a) we studied the kinetics of the polymeric micelles formation stabilized by covalent S-S bonds. Upon thiol-disulfide exchange reaction lipoic acid residues forms intermolecular S-S inside the micelles (it was shown using NMR spectroscopy [38]) accompanied by the particles compactization (the particle size is decreases from 310-330 nm to 240-280 nm), indicating to increased thermodynamic stability (this is a consequence of the decline of the critical micelles concentration). Such micelles compactization results in strengthening of MUTMAC-->R6G FRET (Figure 2b). An appropriate analytical signal here is the I_{550}/I_{450} index (acceptor fluorescence / donor fluorescence) - the effectiveness of FRET effect. The kinetic curve of this I_{550}/I_{450} index shows a minimum at 3-5 minutes (Figure 2b insert), corresponding to the ignition of the donor (MUTMAC in the hydrophobic environment of micelles, and subsequent linear growth up to 1 hour of observation, due to inclusion of FRET probes in the micelle core and prolong process of compactification of micelles during the formation of disulfide bonds

Thus, we have presented 2 pairs of FRET probes that allow us to monitor the formation of micellar structures from surfactants or the kinetics of polymers self-assembling in real time.

Preprints (www.preprints.org) | NOT PEER-REVIEWED | Posted: 6 December 2023 doi:10.20944/preprints202312.0409.v1

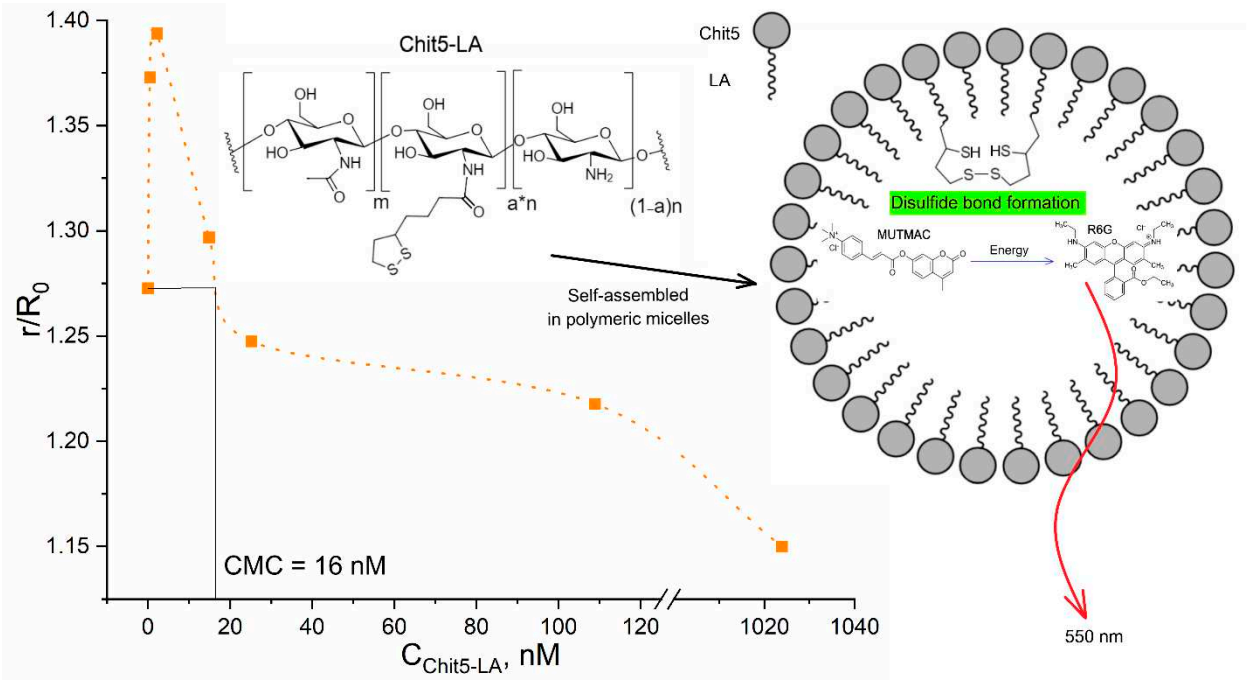

(a)

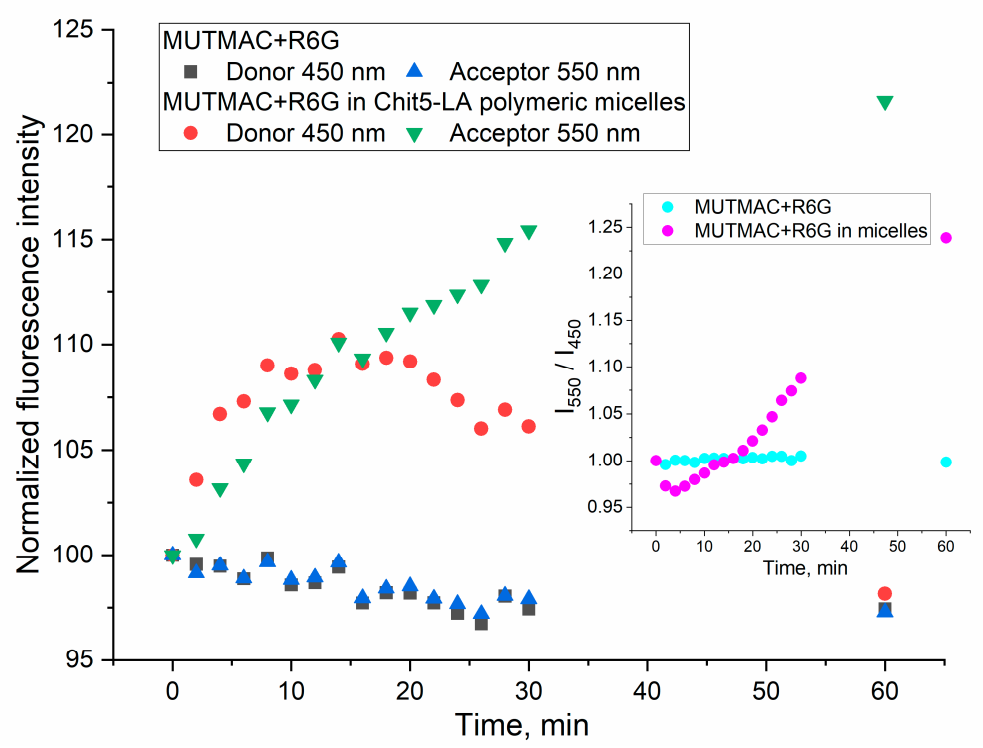

(b)

Figure 2. (a) The dependence of r/R_0 (MUTMAC-R6G) on the Chit5-LA self-assembled molecules concentration. r is the distance between donor and acceptor and R_0 is Förster radius. The excitation wavelength is 360 nm. PBS buffer solution (0.01M, pH 7.4). **(b)** Kinetic fluorescence curves of FRET probe components in buffer solution and during the formation of S-S bonds between crosslinking molecules of Chit5-LA. T = 37 °C.

Preprints (www.preprints.org) | NOT PEER-REVIEWED | Posted: 6 December 2023 doi:10.20944/preprints202312.0409.v1

3.3. Determination of the fluorophore inclusion degree in micelles by enzymatic activity

A complementary approach to FRET probes technique to determine the fluorophore loading degree into the micelles and also the micelle formation (CMC also) is by enzyme catalytic activity. α-Chymotrypsin (proteinase) catalyzes the hydrolysis reaction of MUTMAC to 4-methylumbelliferon (MUmb) (Figure 3) accompanied by the ignition of fluorescence at 450 nm (MUmb fluorescence). Upon formation of the micellar structures from Zephirol, MUTMAC gets inside, into the hydrophobic core, therefore it becomes inaccessible for enzymatic reactions. Thus, with an increase in the surfactant concentration, there would observe a decrease in the apparent reaction rate due to a decrease in the effective concentration of the substrate in aqueous phase.

According to the values of the fluorescence intensity changes at 450 nm (initial splash, which corresponds to the release MUmb product), and in comparison, with an aqueous solution it is possible to judge the amount of fluorophore loaded into the micelle core: 20% of the fluorophore was screened by the surfactant at $C_{zephirol}$ 0.01 mg/mL, and 65% was loaded in the micelles at $C_{zephirol}$ = 0.1 mg/mL. The estimated CMC value calculated using the enzyme technique is 0.25 mM (= 0.1 mg/mL), close to those given in Table 1 obtained using FRET probes approach (R6G with MUTMAC and FITC). It is worth noting that the surfactant can cause denaturation of the enzyme after 1-2 min (in the case of chymotripsin) (Figure 3), therefore, the initial reaction rate can be used as relevant analytical signal.

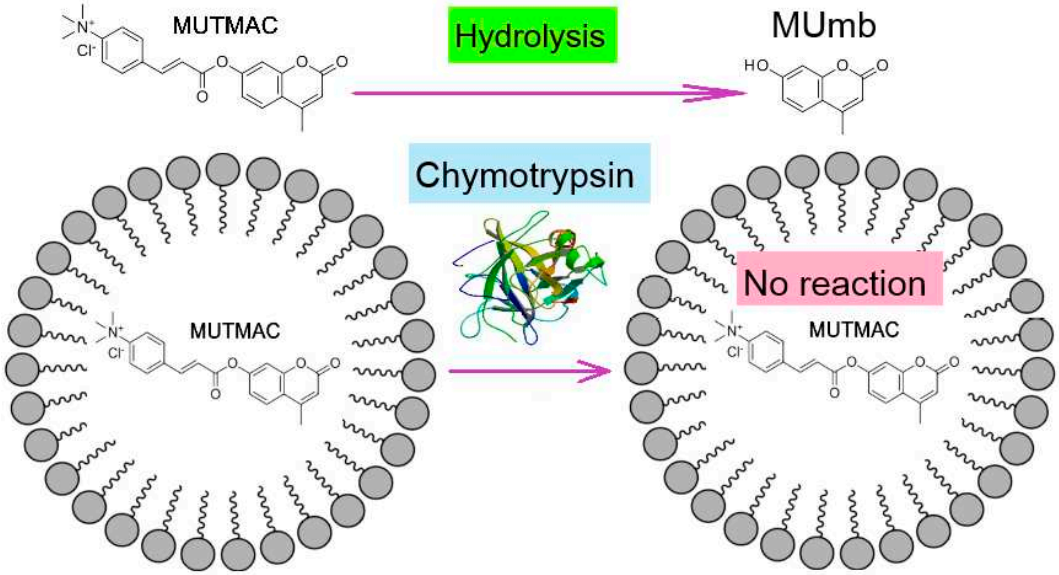

(a)

Preprints (www.preprints.org) | NOT PEER-REVIEWED | Posted: 6 December 2023 doi:10.20944/preprints202312.0409.v1

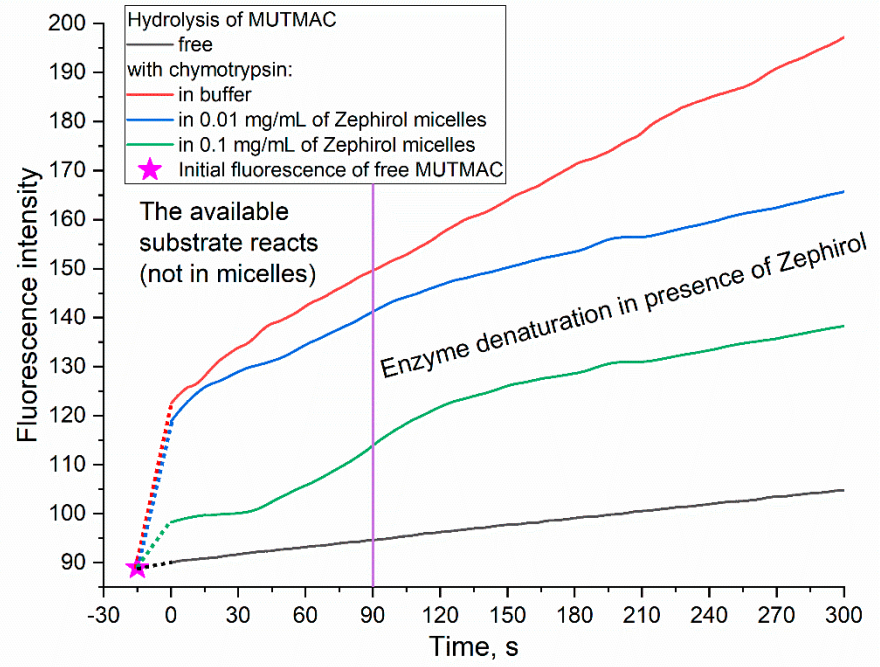

(b)

Figure 3. (a) Experiment design: determination of the fluorophore inclusion degree in micelles by enzymatic activity. **(b)** Kinetic curves of MUTMAC (0.1 mM) hydrolysis in the presence/absence of chymotrypsin (0.4 μM) and various concentrations of zephirol. λ_{exci} = 360 nm, λ_{emi} = 450 nm. PBS (0.01M, pH 7.4). T = 37 °C. The reaction rate was determined by the initial spike in the fluorescence intensity of the product, and not by the tangent of the tilt angle, since the enzyme is partially denatured. The purple vertical line indicates >10% denaturation of the enzyme.

3.4. Studying of the enzyme catalytic activity using FRET probes

FRET probes are further applied to study the enzymatic activity in the membrane-like systems such as reverse micelles. While in classical surfactant micelles, enzymes tend to denature, the use of reversed micelles makes it possible to solubilize enzymes while maintaining or even enhancing their catalytic activity [44–48].

Reverse micelles spontaneously form in a tertiary system containing surfactant, water and non-polar organic solvent. The size of the inner cavity of micelles where protein molecules and other hydrophilic molecules can be entrapped can be strictly controlled by varying the surfactant hydration degree (W_0), which represents the molar ratio of water to surfactant. Reverse micelles can be considered as a "nanoreactor" of molecular size where one can obtain the desired supramolecular form of the protein or its complexes by controlling of the micellar inner cavity size. The method therefore provides the modulation of the enzyme activity and oligomeric composition, as it has been demonstrated for a number of enzymes of different classes [44–48].

This approach is perspective to study the membrane enzymes functioning details and to determine the influence of the membrane lipid compositions on the catalytic activity. For example, the reverse AOT micelles are relevant models of mitochondrial membranes. It is known that the mitochondrial membranes contain non-bilayer lipid structures consisting of associates of lipid molecules arranged as reverse micelles incorporated between monolayers of the bilayer membrane. Water–AOT–isooctane is one of the most intensively studied reverse micellar systems for membrane-protein studying [44–48]. Additionally, reversed AOT-octane micelles are often used to study enzymatic activity to investigate catalytic processes in non-aqueous media and to synthesize or analyze hydrophobic substances. However, in such complex systems due to high background level, low fluorophore quantum yield, unsuitable observation wavelength that interferes with other

 doi:10.20944/preprints202312.0409.v1

components of the system, special conditions are required to selective product detection, such as high sensitivity and signal selectivity. This can be achieved with FRET approach developing here. With this in mind, we applied FRET approach to study the enzyme activity in reverse micelles. Here we consider chymotrypsin, acid and alkaline phosphatase and L-asparaginase as model enzymes catalyzing MUmb or coumarin derivatives with the release of MUmb/coumarin - fluorophores.

FRET is observed in aqueous solution for between MUmb- derivative and R6G, but the FRET effect is rather weak (Figure 1a–c), since the donor and acceptor molecules separated from each other in the volume of the solution. A different situation is observed for reverse micellar system, where the enzyme and the reaction components are located in a limited volume of the aqueous phase of the inner cavity of the micelles.

Convenient for a number of enzymes, the fluorescent substrate based on the MUmb derivatives. During their enzymatic hydrolysis, the fluorescent product MUmb is released, which is reflected in an increase in fluorescence (at 450 nm). This effect can be visualized and amplified by FRET. I.e., the enzymatic reaction can be monitored not only by product (used here as the controle system), but by ascending fluorescence of rhodamine (aceptor) – at 550 nm wavelength. In reversed micelles, FRET is expected to be more pronounced, due to concentration of the enzyme and the reaction components: MUmb will be closer to the acceptor R6G, r/R_0 is decreased, the effectivity of the FRET (E) is greater.

3.4.1. FRET enhancing due to Chymotrypsin activity in AOT-octane reverse micelles

The enzymatic activity of chymotrypsin in reversed micelles by accumulation of the initial product (MUmb) and by increase in the fluorescence intensity of R6G- acceptor due to FRET effect was studied. In AOT-octane reversed micelles, an optimum activity (determined by the enzyme molecule size) for chymotrypsin is observed at the degree of hydration $W_0 = 11$ [46]. Chymotrypsin catalyzes the hydrolysis reaction of MUTMAC to MUmb (Figure 4) in the reversed micellse. It turned out that the enzymatic activity at a wavelength of 450 nm (assigned to MUmb) characterized by low sensitivity, since the fluorescence of the product is strongly quenched in octane. If the FRET effect is realized by including of fluorophore acceptor R6G in the reversed micelles, the sensitivity of the signal increases sharply due to the high quantum yield in the case of R6G. This is due to more than an order of magnitude higher molar emission coefficient of R6G compared to MUmb. Figure 4 shows kinetic curves: hydrolysis of MUTMAC in the presence of R6G compared to background of R6G. The rate of the enzymatic reaction (the tangents of the slope angles of the linear sections of the kinetic curves) are shown in Figure 4 (right insert). The background (without MUTMAC) is about 0.05 units, and the target signal is 0.23, and increased with increasing the R6G concentration., Such a bright FRET effect (an increase in the rhodamine signal) was not observed in control queous buffer solution system. In reversed micelles, a 3-4-fold increase in the initial reaction rate (dI/dt) (by R6G fluorescence signal) upon enzymatic MUmb (donor) release was observed as compared to aqueous system (Figure 4 right insert).

Preprints (www.preprints.org) | NOT PEER-REVIEWED | Posted: 6 December 2023 doi:10.20944/preprints202312.0409.v1

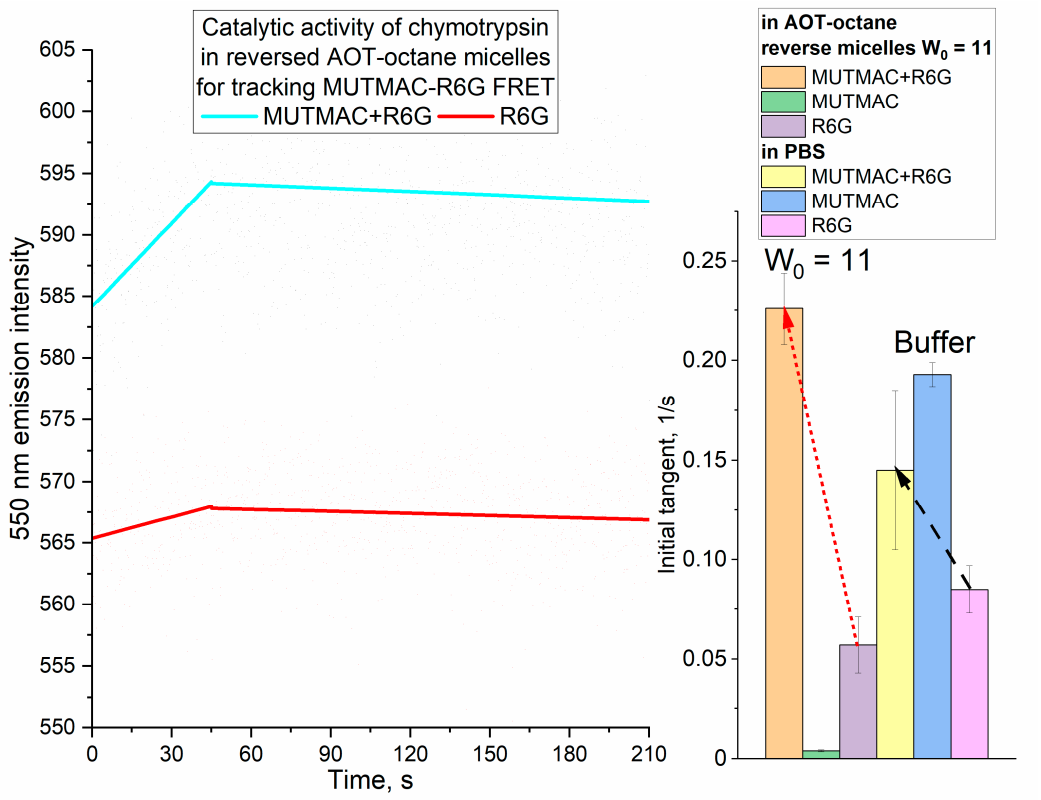

Figure 4. Kinetic curves of MUTMAC (0.2 mM), R6G (2 μM) and its mixture (100/1 mol/mol) hydrolysis in the presence of chymotrypsin (1.5 μM). λ_{exci} = 360 nm, λ_{emi} = 550 nm. AOT/octane reverse micelles. W_0 = 11. PBS (0.01M, pH 7.4). T = 37 °C. Insert on the right: increase in the initial reaction rate (dI/dt) (by R6G fluorescence signal) upon enzymatic MUmb (donor) release is observed for AOT/octane reverse micelles compared to aqueous system.

3.4.2. Acid phosphatase activity in buffer solution and in AOT-octane reverse micelles

It is interesting to explore this phenomenon of the enhancement of FRET effect in the reversed micelles system for a membranotropic enzyme that functions in interaction with a micellar matrix compared with aqueous solution. Therefore, we chose acid phosphatase (membrane enzyme, hydrolase) as a model enzyme, which also (as chymotrypsin) releases the product MUmb during the enzymatic reaction. forming a donor-acceptor pair with R6G.

The dependence of the maximum rate of hydrolysis of 4-methylumbelliferyl phosphate (MUmb-phosphate) catalyzed by acid phosphatase in the system of reversed AOT cells on the degree of hydration of surfactants is a profile with two optima of enzyme activity at hydration degrees W_0 = 20 and 23-25 (Figure 5a). According to the principle of geometric correspondence, the optima of catalytic activity correspond to the coincidence of the size of the protein of the inner cavity of the micelle. Sedimentation analysis of the micellar system showed that at the degree of hydration 20, the enzyme functions as a monomer (48 kDa), and at W_0 = 24 as a dimer (98 kDa). At W_0 = 40, acid phosphatase can form tetramers and complexes with large organic molecules [45].

Figure 5 shows the profiles of phosphatase activity of acid phosphatase in the acetate buffer and in reversed micelles with hydration degrees W_0 = 20, 24 and 40. Detection was carried out by increasing the fluorescence of the initial reaction product (MUmb-phosphate -> MUmb) and by using the FRET- acceptor agent - R6G.

In an aqueous solution, there is no special need for R6G: the rraction rate dI/dt = 240 (Figure 5b,c), and only marginal energy is transmitted to R6G, that is, about 4% (Figure 5c). But in reversed micelles (W_0 = 40), the product signal (MUmb at 450 nm) is strongly extinguished, on the contrary

Preprints (www.preprints.org) | NOT PEER-REVIEWED | Posted: 6 December 2023 doi:10.20944/preprints202312.0409.v1

R6G fluoresces intensively. With a decrease in the hydration degree (micellar size), the fluorescence of MUmb decreases to about 10 times due to quenching, but FRET effect is still pronounced.

The observed rate of the enzymatic reaction tracked by R6G depends on the size of the reversed micelles. At W_0 = 20 or 24, about 10% of the fluorescence signal (velocity dI/dt) passes to R6G, and at W_0 = 40, about 13% of velocity is transferred to rhodamine. This is due to optimal size of the inner aqueous phase in the micelles: including places for enzyme, substrate and R6G. Thus, the observed dependence of the energy transfer efficiency to R6G on the product has a minimum at W_0 38-42. With high hydration degrees, we gradually approach to the situation in an aqueous solution, and with low degrees of hydration, the micelles have too small an internal cavity to accommodate the optimal amount of substrate and FRET agent (R6G)

It is worth noting here that the FRET agent is used in a deficit (100-500 fold) to obtain comparable fluorescence values. It is possible to increase the amount of R6G, thereby significantly increasing the analytical signal and reducing the required amounts of substrate and enzyme. With an increase in the concentration of rhodamine by 5 and 20 times, the observed rate of enzymatic reaction tracked by rhodamine increases by 2.5 and 6 times, respectively. In addition, the shift to the long-wavelength region increases the selectivity of the signal.

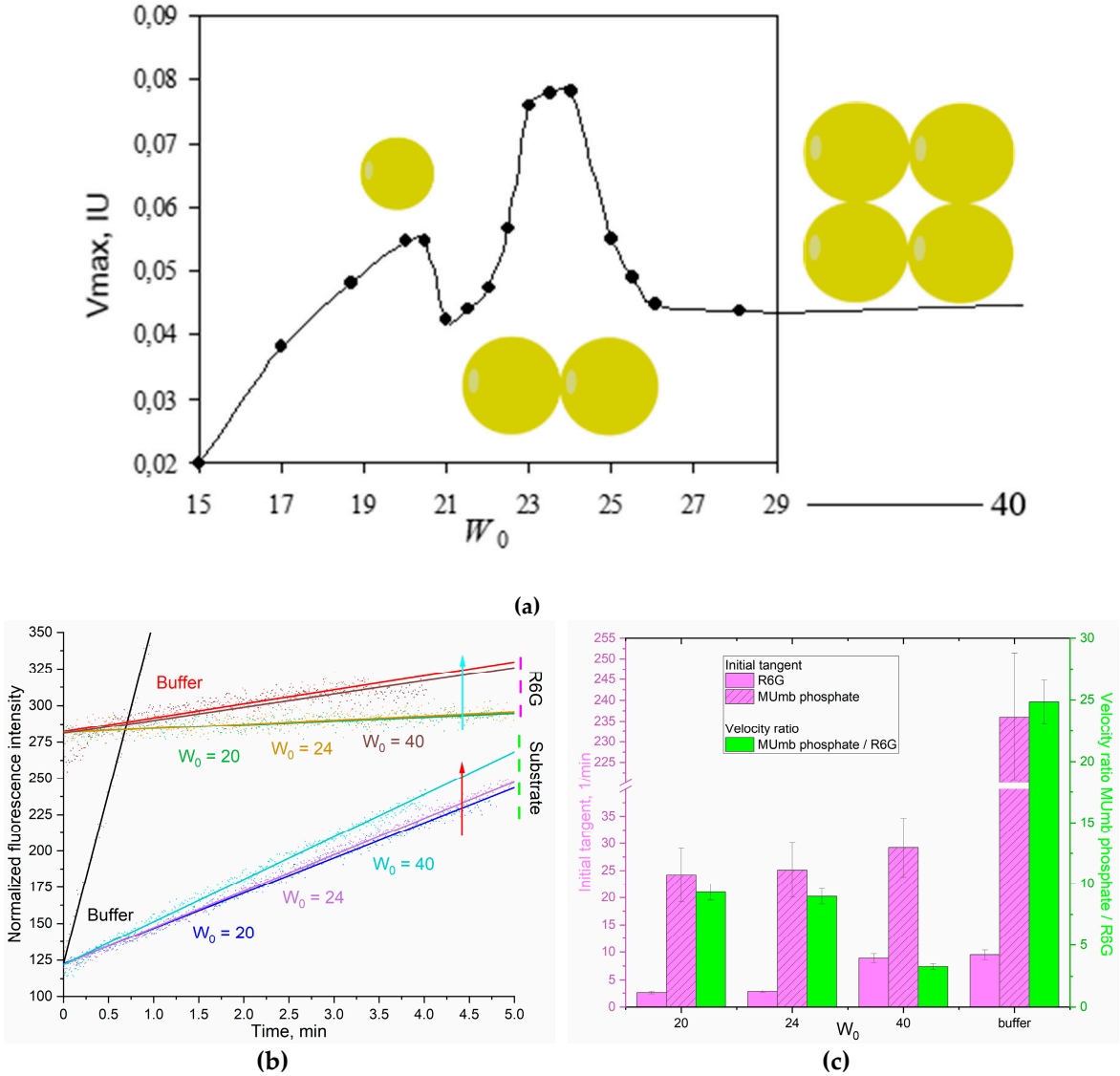

Figure 5. (a) The dependence of the catalytic activity (V_{max}) of acid phosphatase (1 μM) on the hydration degree of AOT (W_0) in the reversed micelles system. KOAc/HOAc (0.01M, pH 4.9). T = 37 °C. **(b)** Phosphatase activity profiles curves of acid phosphatase (1 μM) in relation to MUmb-

Preprints (www.preprints.org) | NOT PEER-REVIEWED | Posted: 6 December 2023 doi:10.20944/preprints202312.0409.v1

phosphate (0.8 mM) with FRET agent R6G-acceptor (2 μM). λ_{exci} = 360 nm, λ_{emi} = 450 (substrate – MUmb-phosphate and product – MUmb), 550 (R6G) nm. AOT/octane reverse micelles. W_0 = 20, 24, 40. KOAc/HOAc (0.01M, pH 4.9). T = 37 °C. **(c)** Tangents of the initial linear sections of phosphatase profiles, the ratio of the initial "velocities" of the observed signals for the product and for the FRET agent R6G.

3.4.3. Catalytic activity in a two-enzyme system: alkaline phosphatase and asparaginase

Acid phosphatase functions at slightly acidic pH values (about 5.0 – jvdel for the tumor cells microenvirinment), but it is important to study the FRET effect also in neutral – weakly alkaline pH (normal cells model). To do this, we used alkaline phosphatase and asparaginase with pH optimum of about 8.0. Further FRET probe was used to study the catalytic activity in a two-enzyme system.

Indeed, in the research practice in biochemistry there is often a need to study enzymatic reactions in two-enzyme systems: to increase the sensitivity of the signal, to study the mutual influence in the composition of enzyme complexes, to study successive enzymatic reactions, the effect of inhibition in biochemistry, etc. We suggest to study such reactions using FRET approacj developed here. This may be the parallel accumulation of one fluorophore donor or the accumulation of two consecutive fluorescence donors.

We chose asparaginase and alkaline phosphatase as model enzymes. For example, it would be useful to follow the asparaginase avtivity by rhodamine when analyzing the activity of asparaginase in the blood serum samples of patients in the treatment of leukemia. Asparaginase hydrolyzes the fluorescent substrate L-aspartic acid β-(7-amido-4-methylcoumarin) to aspartate and coumarin derivative, and alkaline phosphatase hydrolyzes MUmb-phospate to MUmb (Figure 6a). The activity of the enzymes was studied in two enzyme systems with a hydration degree W_0 = 40, since both enzymes are quite active at such a W_0, and can be located in one micelle.

Figure 6 shows the kinetic curves of the enzymatic activity of asparaginase, alkaline phosphatase and their mixed system. The initial linear sections are identified, from which the initial reaction rate can be determined (dI/dt), by inital products as well as by R6G fluorescense increase. Table 2 shows the parametr dI/dt of the initial linear region of kinetic curves.

In the case of asparaginase, approximately 20% of the $(dI/dt)_{product}$ passes to R6G. For alkaline phosphatase, this FRET characteristic is a bit lower and equal to about 15%. In a two-enzyme system, the efficiency of FRET is in the range of 15-20%. Thus, we were able to monitor the enzymatic reactions of hydrolysis using R6G. In general, the obtained data are promising for practical applications in enzymological studies and visualization of processes in the cell using confocal microscopy to reduce autofluorescence.

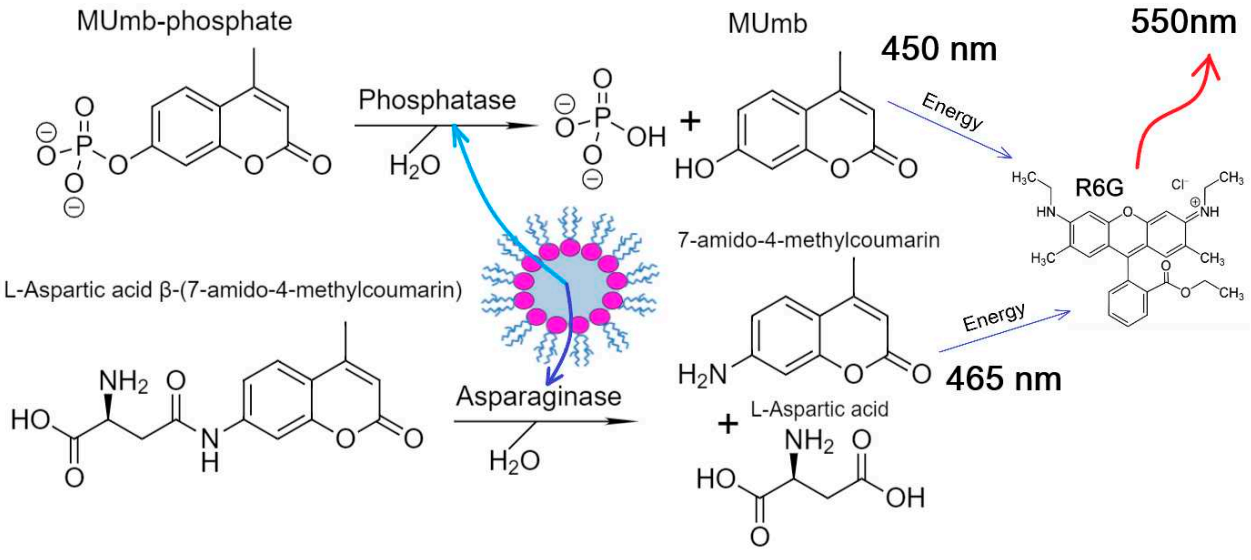

(a)

Preprints (www.preprints.org) | NOT PEER-REVIEWED | Posted: 6 December 2023 doi:10.20944/preprints202312.0409.v1

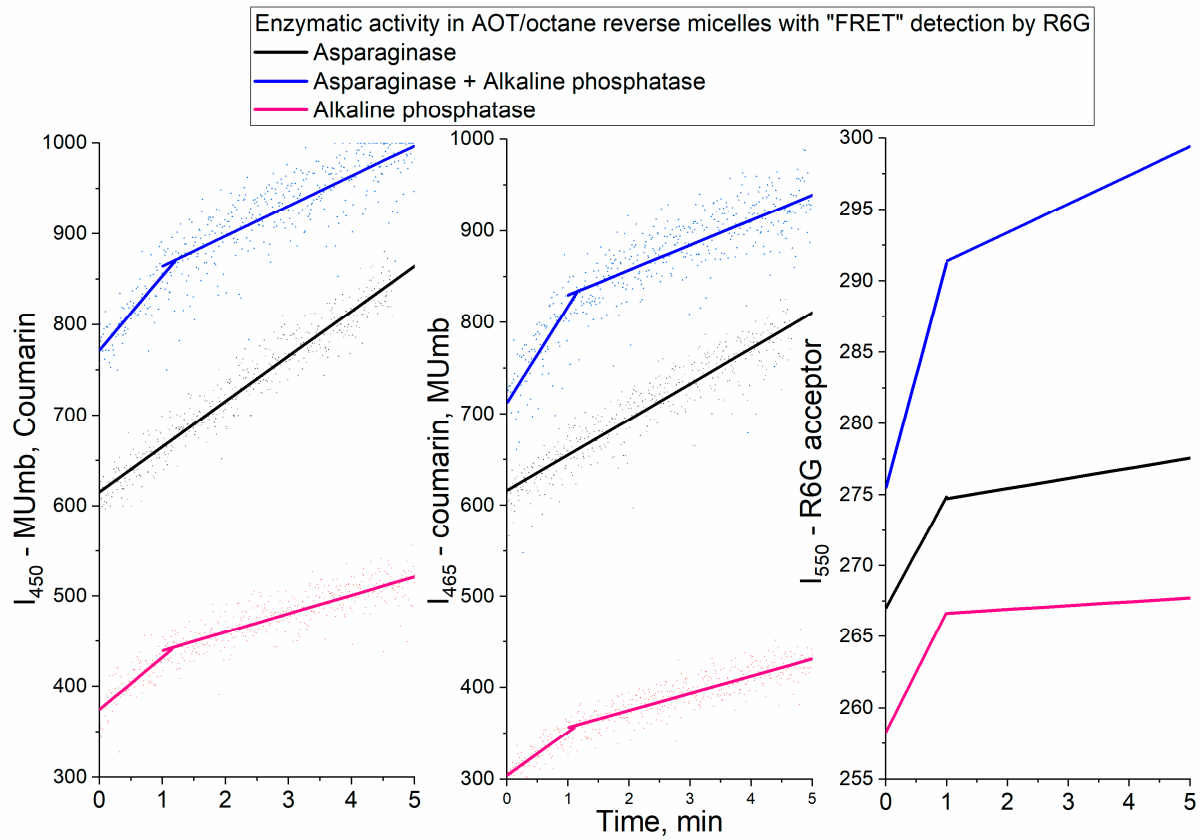

(b)

Figure 6. (a) Experiment design: Catalytic activity in a two-enzyme system: alkaline phosphatase and asparaginase. **(b)** Activity profiles curves of alkaline phosphatase (1 μM), asparaginase (1 μM) in relation to MUmb-phosphate (0.2 mM) and L-Aspartic acid β-(7-amido-4-methylcoumarin) (0.2 mM), correspondingly, with FRET agent R6G-acceptor (2 μM). λ_{exci} = 360 nm, λ_{emi} = 450 nm (product 1 – MUmb), 465 (product 2 –coumarin derivative), 550 nm (R6G – FRET agent). AOT/octane reverse micelles, W_0 = 40. Na-phosphate buffer (0.02M, pH 8.2). T = 37 °C.

Table 2. Initial tangents of the linear fragments of asparaginase and phosphatase kinetic profiles. AOT/octane reverse micelles, W_0 = 40. Na-phosphate buffer (0.02M, pH 8.2). T = 22 °C.

Enzyme / Emission wavelength	Initial tangent, 1/min		
	450 nm (MUmb > coumarin)	465 nm (Coumarin > MUmb)	550 nm (R6G)
Asparaginase	50±1	39±1	7.9±0.3
Alkaline phosphatase	57±4	48±4	8.4±0.5
Asparaginase + Alkaline phosphatase	82±6	105±7	16±1

Thus, using the examples of four enzymes, we have shown that it is possible to study catalysis using a FRET probe (R6G-acceptor), which makes it possible to significantly increase the anatomical signal and enhance its selectivity by shifting to the red region. In addition, the proposed methods are promising for use as visualizers of cellular structures and on-line reactions.

4. Conclusions

In this paper, we proposed the use of the FRET probe technique (R6G with FITC or methylumbelliferon derivatives) as an indicator of micelle formation from surfactants, chitosan grafted with fatty acid, as well as to study enzymatic activity by fluorescence signal from R6G

obtained by FRET. In relation to surfactants (anionic SDS, cationic Zephirol and non-ionic Triton X-100), the FRET probe technique provides valuable information about the distance of the donor and acceptor fluorophores r/R_0, which can be used to study the mechanism of micelle formation and determine the composition of the system (individual molecules/pre-micelles/micelles), and there is also calculation of CMC. Using a FRET probe, we determined the kinetics of S-S crosslinking formation, which is important in the field of stimulus-sensitive drug delivery systems in tumors. The most interesting application of the FRET probe technique turned out to be the possibility of studying the enzymatic activity not by product, but by the FRET between the product of the enzymatic reaction and the R6G acceptor. We have shown that the efficiency of FRET varies from 5 to 20% depending on the composition of the system and the type of enzyme. 4 model enzymes were studied: acidic and alkaline phosphatases, asparaginase and chymotrypsin in aqueous media and systems of reversed AOT–octane micelles. The obtained data are promising in the field of enzymology, as well as visualization of processes in living cells using fluorescent microscopy to increase selectivity and signal intensity.

Supplementary Materials: Figure S1. The scheme of synthesis grafted chitosan with lipoic acid – Chit5-LA. **Figure S2.** (a) AFM image of Chit5-LA particles and (b) the corresponding section along the blue line in height, respectively.

Author Contributions: Conceptualization, E.V.K. and I.D.Z.; methodology, I.D.Z., E.V.K., and I.V.S.; formal analysis, I.D.Z. and I.V.S.; investigation, I.D.Z. and I.V.S.; data curation, I.D.Z.; writing—original draft preparation, I.D.Z. and I.V.S.; writing—review and editing, E.V.K.; project supervision, E.V.K.; funding acquisition, E.V.K. All authors have read and agreed to the published version of the manuscript.

Funding: This research was funded by the Russian Science Foundation, grant number 24-25-00104.

Data Availability Statement: The data presented in this study are available in the main text.

Acknowledgments: The work was performed using the equipment (FTIR microscope MICRAN-3, FTIR spectrometer Bruker Tensor 27, Jasco J-815 CD Spectrometer, AFM microscope NTEGRA II) of the program for the development of Moscow State University.

Conflicts of Interest: The authors declare no conflicts of interest.

Abbreviations

AOT – bis(2-ethylhexyl) sulfosuccinate or dioctyl sulfosuccinate; Chit—chitosan; CMC – critical micelle concentration; CPMC – critical pre-micelle concentration; FITC – fluorescein isothiocyanate; FRET—Förster resonance energy transfer; LA – lipoic acid; MUmb – 4-methylumbelliferone or methylumbelliferyl; MUTMAC – 4-methylumbelliferyl p-trimethylammoniocinnamate chloride; R6G – rhodamine 6G; SDS – sodium dodecyl sulfate; W_0 – degree of hydration of reversed micelles.

References

1. Liao, J.Y.; Song, Y.; Liu, Y. A new trend to determine biochemical parameters by quantitative FRET assays. *Acta Pharmacol. Sin.* **2015**, *36*, 1408–1415, doi:10.1038/aps.2015.82.
2. Bhat, P.A.; Chat, O.A.; Dar, A.A. Exploiting Co-solubilization of Warfarin, Curcumin, and Rhodamine B for Modulation of Energy Transfer: A Micelle FRET On/Off Switch. *ChemPhysChem* **2016**, 2360–2372, doi:10.1002/cphc.201600274.
3. Zhang, H.; Li, H.; Cao, Z.; Du, J.; Yan, L.; Wang, J. Investigation of the in vivo integrity of polymeric micelles via large Stokes shift fluorophore-based FRET. *J. Control. Release* **2020**, *324*, 47–54, doi:10.1016/j.jconrel.2020.04.046.
4. Barros, C.H.N.; Hiebner, D.W.; Fulaz, S.; Vitale, S.; Quinn, L.; Casey, E. Synthesis and self-assembly of curcumin-modified amphiphilic polymeric micelles with antibacterial activity. *J. Nanobiotechnology* **2021**, *19*, 1–15, doi:10.1186/s12951-021-00851-2.
5. Wang, Z.; Deng, X.; Ding, J.; Zhou, W.; Zheng, X.; Tang, G. Mechanisms of drug release in pH-sensitive micelles for tumour targeted drug delivery system: A review. *Int. J. Pharm.* **2018**, *535*, 253–260, doi:10.1016/j.ijpharm.2017.11.003.

6. Le-Vinh, B.; Le, N.M.N.; Nazir, I.; Matuszczak, B.; Bernkop-Schnürch, A. Chitosan based micelle with zeta potential changing property for effective mucosal drug delivery. *Int. J. Biol. Macromol.* **2019**, *133*, 647–655, doi:10.1016/j.ijbiomac.2019.04.081.
7. Parra, A.; Jarak, I.; Santos, A.; Veiga, F.; Figueiras, A. Polymeric micelles: A promising pathway for dermal drug delivery. *Materials (Basel).* **2021**, *14*, doi:10.3390/ma14237278.
8. He, L.; Qin, X.; Fan, D.; Feng, C.; Wang, Q.; Fang, J. Dual-Stimuli Responsive Polymeric Micelles for the Effective Treatment of Rheumatoid Arthritis. *ACS Appl. Mater. Interfaces* **2021**, *13*, 21076–21086, doi:10.1021/acsami.1c04953.
9. Kumar, R.; Sirvi, A.; Kaur, S.; Samal, S.K.; Roy, S.; Sangamwar, A.T. Polymeric micelles based on amphiphilic oleic acid modified carboxymethyl chitosan for oral drug delivery of bcs class iv compound: Intestinal permeability and pharmacokinetic evaluation. *Eur. J. Pharm. Sci.* **2020**, *153*, 105466, doi:10.1016/j.ejps.2020.105466.
10. Jiang, G.B.; Quan, D.; Liao, K.; Wang, H. Preparation of polymeric micelles based on chitosan bearing a small amount of highly hydrophobic groups. *Carbohydr. Polym.* **2006**, *66*, 514–520, doi:10.1016/j.carbpol.2006.04.008.
11. Luo, T.; Han, J.; Zhao, F.; Pan, X.; Tian, B.; Ding, X.; Zhang, J. Redox-sensitive micelles based on retinoic acid modified chitosan conjugate for intracellular drug delivery and smart drug release in cancer therapy. *Carbohydr. Polym.* **2019**, *215*, 8–19, doi:10.1016/j.carbpol.2019.03.064.
12. Almeida, A.; Araújo, M.; Novoa-Carballal, R.; Andrade, F.; Gonçalves, H.; Reis, R.L.; Lúcio, M.; Schwartz, S.; Sarmento, B. Novel amphiphilic chitosan micelles as carriers for hydrophobic anticancer drugs. *Mater. Sci. Eng. C* **2020**, *112*, 110920, doi:10.1016/j.msec.2020.110920.
13. Kost, B.; Brzeziński, M.; Cieślak, M.; Królewska-Golińska, K.; Makowski, T.; Socka, M.; Biela, T. Stereocomplexed micelles based on polylactides with β-cyclodextrin core as anti-cancer drug carriers. *Eur. Polym. J.* **2019**, *120*, 109271, doi:10.1016/j.eurpolymj.2019.109271.
14. Xu, W.; Wang, H.; Dong, L.; Zhang, P.; Mu, Y.; Cui, X.; Zhou, J.; Huo, M.; Yin, T. Hyaluronic acid-decorated redox-sensitive chitosan micelles for tumor-specific intracellular delivery of gambogic acid. *Int. J. Nanomedicine* **2019**, *14*, 4649–4666, doi:10.2147/IJN.S201110.
15. Lin, D.; Xiao, L.; Qin, W.; Loy, D.A.; Wu, Z.; Chen, H.; Zhang, Q. Preparation, characterization and antioxidant properties of curcumin encapsulated chitosan/lignosulfonate micelles. *Carbohydr. Polym.* **2022**, *281*, 119080, doi:10.1016/j.carbpol.2021.119080.
16. Stern, T.; Kaner, I.; Laser Zer, N.; Shoval, H.; Dror, D.; Manevitch, Z.; Chai, L.; Brill-Karniely, Y.; Benny, O. Rigidity of polymer micelles affects interactions with tumor cells. *J. Control. Release* **2017**, *257*, 40–50, doi:10.1016/j.jconrel.2016.12.013.
17. Kim, M.P.; Kim, H.J.; Kim, B.J.; Yi, G.R. Structured nanoporous surfaces from hybrid block copolymer micelle films with metal ions. *Nanotechnology* **2015**, *26*, doi:10.1088/0957-4484/26/9/095302.
18. Kaeokhamloed, N.; Legeay, S.; Roger, E. FRET as the tool for in vivo nanomedicine tracking. *J. Control. Release* **2022**, *349*, 156–173, doi:10.1016/j.jconrel.2022.06.048.
19. Zlotnikov, I.D.; Savchenko, I. V.; Kudryashova, E. V. Fluorescent Probes with Förster Resonance Energy Transfer Function for Monitoring the Gelation and Formation of Nanoparticles Based on Chitosan Copolymers. *J. Funct. Biomater.* **2023**, *14*, doi:10.3390/jfb14080401.
20. Grosso, R.; De-Paz, M.V. Thiolated-polymer-based nanoparticles as an avant-garde approach for anticancer therapies—reviewing thiomers from chitosan and hyaluronic acid. *Pharmaceutics* **2021**, *13*, doi:10.3390/pharmaceutics13060854.
21. Liu, Z.; Jiao, Y.; Wang, Y.; Zhou, C.; Zhang, Z. Polysaccharides-based nanoparticles as drug delivery systems. *Adv. Drug Deliv. Rev.* **2008**, *60*, 1650–1662, doi:10.1016/j.addr.2008.09.001.
22. Harish, R.; Nisha, K.D.; Prabakaran, S.; Sridevi, B.; Harish, S.; Navaneethan, M.; Ponnusamy, S.; Hayakawa, Y.; Vinniee, C.; Ganesh, M.R. Cytotoxicity assessment of chitosan coated CdS nanoparticles for bio-imaging applications. *Appl. Surf. Sci.* **2020**, *499*, 143817, doi:10.1016/j.apsusc.2019.143817.
23. Kievit, F.M.; Veiseh, O.; Bhattarai, N.; Fang, C.; Gunn, J.W.; Lee, D.; Ellenbogen, R.G.; Olson, J.M.; Zhang, M. PEI-PEG-chitosan-copolymer-coated iron oxide nanoparticles for safe gene delivery: Synthesis, complexation, and transfection. *Adv. Funct. Mater.* **2009**, *19*, 2244–2251, doi:10.1002/adfm.200801844.

24. Jin, Y.H.; Hu, H.Y.; Qiao, M.X.; Zhu, J.; Qi, J.W.; Hu, C.J.; Zhang, Q.; Chen, D.W. PH-sensitive chitosan-derived nanoparticles as doxorubicin carriers for effective anti-tumor activity: Preparation and in vitro evaluation. *Colloids Surfaces B Biointerfaces* **2012**, *94*, 184–191, doi:10.1016/j.colsurfb.2012.01.032.
25. Zaki, I.; Moustafa, A.M.Y.; Beshay, B.Y.; Masoud, R.E.; Elbastawesy, M.A.I.; Abourehab, M.A.S.; Zakaria, M.Y. Design and synthesis of new trimethoxylphenyl-linked combretastatin analogues loaded on diamond nanoparticles as a panel for ameliorated solubility and antiproliferative activity. *J. Enzyme Inhib. Med. Chem.* **2022**, *37*, 2679–2701, doi:10.1080/14756366.2022.2116016.
26. Chaubey, P.; Mishra, B.; Mudavath, S.L.; Patel, R.R.; Chaurasia, S.; Sundar, S.; Suvarna, V.; Monteiro, M. Mannose-conjugated curcumin-chitosan nanoparticles: Efficacy and toxicity assessments against Leishmania donovani. *Int. J. Biol. Macromol.* **2018**, *111*, 109–120, doi:10.1016/j.ijbiomac.2017.12.143.
27. Fuenzalida, J.P.; Weikert, T.; Hoffmann, S.; Vila-Sanjurjo, C.; Moerschbacher, B.M.; Goycoolea, F.M.; Kolkenbrock, S. Affinity protein-based FRET tools for cellular tracking of chitosan nanoparticles and determination of the polymer degree of acetylation. *Biomacromolecules* **2014**, *15*, 2532–2539, doi:10.1021/bm500394v.
28. Divya, K.; Jisha, M.S. Chitosan nanoparticles preparation and applications. *Environ. Chem. Lett.* **2018**, *16*, 101–112, doi:10.1007/s10311-017-0670-y.
29. Yadav, P.; Yadav, A.B. Preparation and characterization of BSA as a model protein loaded chitosan nanoparticles for the development of protein-/peptide-based drug delivery system. *Futur. J. Pharm. Sci.* **2021**, *7*, doi:10.1186/s43094-021-00345-w.
30. Woranuch, S.; Yoksan, R. Eugenol-loaded chitosan nanoparticles: I. Thermal stability improvement of eugenol through encapsulation. *Carbohydr. Polym.* **2013**, *96*, 578–585, doi:10.1016/j.carbpol.2012.08.117.
31. Cho, K.; Wang, X.; Nie, S.; Chen, Z.; Shin, D.M. Therapeutic nanoparticles for drug delivery in cancer. *Clin. Cancer Res.* **2008**, *14*, 1310–1316, doi:10.1158/1078-0432.CCR-07-1441.
32. Alizadeh, D.; Zhang, L.; Hwang, J.; Schluep, T.; Badie, B. Tumor-associated macrophages are predominant carriers of cyclodextrin-based nanoparticles into gliomas. *Nanomedicine Nanotechnology, Biol. Med.* **2010**, *6*, 382–390, doi:10.1016/j.nano.2009.10.001.
33. Tripathy, S.K.; Yu, Y.T. Spectroscopic investigation of S-Ag interaction in ω-mercaptoundecanoic acid capped silver nanoparticles. *Spectrochim. Acta - Part A Mol. Biomol. Spectrosc.* **2009**, *72*, 841–844, doi:10.1016/j.saa.2008.12.004.
34. Dobryakova, N. V.; Zhdanov, D.D.; Sokolov, N.N.; Aleksandrova, S.S.; Pokrovskaya, M. V.; Kudryashova, E. V. Improvement of Biocatalytic Properties and Cytotoxic Activity of L-Asparaginase from Rhodospirillum rubrum by Conjugation with Chitosan-Based Cationic Polyelectrolytes. *Pharmaceuticals* **2022**, *15*, doi:10.3390/ph15040406.
35. Dobryakova, N. V.; Zhdanov, D.D.; Sokolov, N.N.; Aleksandrova, S.S.; Pokrovskaya, M. V.; Kudryashova, E. V. Rhodospirillum rubrum L-Asparaginase Conjugates with Polyamines of Improved Biocatalytic Properties as a New Promising Drug for the Treatment of Leukemia. *Appl. Sci.* **2023**, *13*, doi:10.3390/app13053373.
36. Zlotnikov, I.D.; Streltsov, D.A.; Ezhov, A.A.; Kudryashova, E. V. Smart pH- and Temperature-Sensitive Micelles Based on Chitosan Grafted with Fatty Acids to Increase the Efficiency and Selectivity of Doxorubicin and Its Adjuvant Regarding the Tumor Cells. *Pharmaceutics* **2023**, *15*, doi:10.3390/pharmaceutics15041135.
37. Zlotnikov, I.D.; Streltsov, D.A.; Belogurova, N.G.; Kudryashova, E. V. Chitosan or Cyclodextrin Grafted with Oleic Acid Self-Assemble into Stabilized Polymeric Micelles with Potential of Drug Carriers. *Life* **2023**, *13*, doi:10.3390/life13020446.
38. Zlotnikov, I.D.; Ezhov, A.A.; Ferberg, A.S.; Krylov, S.S.; Semenova, M.N.; Semenov, V. V.; Kudryashova, E. V. Polymeric Micelles Formulation of Combretastatin Derivatives with Enhanced Solubility, Cytostatic Activity and Selectivity against Cancer Cells. *Pharmaceutics* **2023**, *15*, doi:10.3390/pharmaceutics15061613.
39. Zlotnikov, I.D.; Vigovskiy, M.A.; Davydova, M.P.; Danilov, M.R.; Dyachkova, U.D.; Grigorieva, O.A.; Kudryashova, E. V. Mannosylated Systems for Targeted Delivery of Antibacterial Drugs to Activated Macrophages. *Int. J. Mol. Sci.* **2022**, *23*, 1–29, doi:10.3390/ijms232416144.
40. Bales, B.L.; Messina, L.; Vidal, A.; Peric, M.; Nascimento, O.R. Precision relative aggregation number determinations of SDS micelles using a spin probe. A model of micelle surface hydration. *J. Phys. Chem. B* **1998**, *102*, 10347–10358, doi:10.1021/jp983364a.

41. Robson, R.J.; Dennis, E.A. The size, shape, and hydration of nonionic surfactant micelles. Triton X-100. *J. Phys. Chem.* **1977**, *81*, 1075–1078, doi:10.1021/j100526a010.
42. Wu, S.; Liang, F.; Hu, D.; Li, H.; Yang, W.; Zhu, Q. Determining the Critical Micelle Concentration of Surfactants by a Simple and Fast Titration Method. *Anal. Chem.* **2020**, *92*, 4259–4265, doi:10.1021/acs.analchem.9b04638.
43. Deutschle, T.; Porkert, U.; Reiter, R.; Keck, T.; Riechelmann, H. In vitro genotoxicity and cytotoxicity of benzalkonium chloride. *Toxicol. Vitr.* **2006**, *20*, 1472–1477, doi:10.1016/j.tiv.2006.07.006.
44. Kudryashova, E. V.; Leferink, N.G.H.; Slot, I.G.M.; Van Berkel, W.J.H. Galactonolactone oxidoreductase from Trypanosoma cruzi employs a FAD cofactor for the synthesis of vitamin C. *Biochim. Biophys. Acta - Proteins Proteomics* **2011**, *1814*, 545–552, doi:10.1016/j.bbapap.2011.03.001.
45. Kudryashova, E. V.; Bronza, V.L.; Vinogradov, A.A.; Kamyshny, A.; Magdassi, S.; Levashov, A. V. Regulation of acid phosphatase in reverse micellar system by lipids additives: Structural aspects. *J. Colloid Interface Sci.* **2011**, *353*, 490–497, doi:10.1016/j.jcis.2010.09.072.
46. Creagh, A.L.; Prausnitz, J.M.; Blanch, H.W. Structural and catalytic properties of enzymes in reverse micelles. *Enzyme Microb. Technol.* **1993**, *15*, 383–392, doi:10.1016/0141-0229(93)90124-K.
47. Maitra, A.; Ghosh, P.K.; De, T.K.; Sahoo, S.K. Process for the preparation of highly monodispersed polymeric hydrophilic nanoparticles. **1997**, 5.
48. Maitra, A.; Ghosh, P.K.; De, T.K.; Sahoo, S.K. Process for the preparation of highly monodispersed polymeric hydrophilic nanoparticles. **1997**, 5.